Genesis of the Antarctic Slope Current in West Antarctica

Andrew F. Thompson^{1,*}, Kevin G. Speer², and Lena M. Schulze Chretien³

- ¹California Institute of Technology, Environmental Science and Engineering, Pasadena, CA 91125, USA
- ²Geophysical Fluid Dynamics Institute, and Department of Earth, Ocean, and Atmospheric Science, Florida State University, Tallahassee, Florida
- ³Marine Science Research Institute, Jacksonville University, 2800 University Blvd N, Jacksonville, FL 32211, USA *andrewt@caltech.edu

ABSTRACT

The stability of the West Antarctic ice sheet (WAIS) depends on the supply of heat to its base and remains a major source of uncertainty in future predictions of sea level rise. The delivery of heat towards floating Antarctic ice shelves depends on water properties that are set by transport and mixing processes over the continental slope and shelf. The Antarctic Slope Current (ASC), a major boundary current of the ocean's global circulation, serves as a dynamic gateway for heat transport towards Antarctica, isolating a large part of the continent, to some extent, from warm deep water. Here, we use observations collected from the sparsely-sampled Bellingshausen Sea to propose a mechanistic explanation for the initiation of the westward-flowing ASC. Modified water masses found in the Bellingshausen Sea show the signature of formation through ocean-sea-ice and ocean-ice-shelf interactions. A narrow, topographically-steered western boundary current in the Bellingshausen Sea focuses the outflow of these modified waters and produces a localized front at the shelf break that supports the emerging ASC. This mechanism emphasizes the importance of buoyancy forcing, integrated over the continental shelf, as opposed to local wind forcing, in the generation mechanism. The ASC's westward flow can transport water properties towards the Amundsen Sea and farther downstream, suggesting the potential for remote control of melt rates of the WAIS' largest ice shelves.

Introduction

Floating ice shelves throughout West Antarctica buttress ice sheets that hold the equivalent of 3.2 m of global sea level rise. Over recent decades, these ice shelves have thinned¹, largely in response to melting from below by warm ocean waters^{2,3}. This warm water is sourced from the Circumpolar Deep Water (CDW) water mass found off the continental shelf⁴. Variability in the poleward transport of heat, largely thought to be influenced by the thickness of the CDW layer⁵, has been attributed to local wind forcing⁶, ice shelf melt⁷, and surface forcing over the continental shelf⁸. Transport and mixing processes at the shelf break set the properties of the warm water as it moves on to the shelf⁹, and strong gradients in water properties here are referred to as the Antarctic Slope Front (ASF)^{4,10}. This front supports the dominant circulation feature over the continental slope, the Antarctic Slope Current^{9,10}, that governs along- and across-slope transport rates¹¹.

The ASC is a persistent westward-flowing (prograde) circulation feature around most of Antarctica. Along the West Antarctic Peninsula (WAP), however, flow at the shelf break is eastward (retrograde), associated with the southern limit of the

Antarctic Circumpolar Current (ACC). Here, CDW extends to the shelf break and a modified (slightly colder) form, MCDW, is shed on to the shelf as eddies¹². In contrast, observations indicate a westward slope current in the Amundsen Sea, which may be modulated by an eastward undercurrent^{13, 14}. This implies that the Bellingshausen Sea (BellS) sector marks a transition in the circulation structure over the slope. In this region, the southern-most extent of the ACC, the eastern boundary of the Ross Gyre, and the shelf circulation are all in close proximity^{14, 15}.

The formation and persistence of the ASF and ASC is traditionally attributed to surface wind forcing ^{10,16} or tides ¹⁷. Shoreward Ekman transport due to easterly winds, which dominate the surface forcing over most of the Antarctic slope, establishes a geostrophically-balanced along-slope flow in the direction of the wind stress. Ekman pumping or dense shelf water may induce baroclinic shear that modifies the vertical structure of the ASC^{18,19}. However, the Amundsen Sea low-pressure system in West Antarctica causes the WAP, Bellingshausen and Amundsen Seas to experience the weakest along-slope winds of the Antarctic margins, with a mean along-slope wind stress of only -0.01 N m^{-2 20,21} (Supp. Figure 1). Despite this weak forcing, observations²² and numerical models¹⁵ provide strong support for a westward-flowing current above the slope at the western limit of the Bellingshausen Sea. This westward flow is not associated with the traditional, wind-forced, formation mechanism of the ASF, and it has not previously been related to the ASC.

Water properties entering the eastern Amundsen Sea flow towards the major ice shelves associated with the Pine Island and Thwaites glaciers^{14,23} and may influence their melt rates. Hence the genesis of westward flow in the Bellingshausen Sea is a missing link in the chain of Antarctic ocean-ice interactions. In addition to supporting inter-sea exchange of water properties, the structure of the ASC modulates the temperature, thickness and volume transport of warm CDW to ice shelves experiencing basal melt throughout West Antarctica. Finally, ASC transport estimates indicate that this current can reach tens of Sverdrups^{24–26}, a magnitude comparable to the ocean's global meridional overturning circulation. If the ASC source intersects the ACC in this region, then the former becomes a major component of the overturning circulation itself, in a dramatic three-dimensional network. The ASC then contributes to the redistribution of glacially-modified waters longitudinally to sites of dense water mass transformation, helping to close the southern limb of the global overturning circulation²⁷.

Results

Hydrography of the Bellingshausen Sea

In this study, we analyze hydrographic observations collected from two research cruises in the BellS, JR165 in 2007 and NBP19-01 in 2019 (Figure 1) as well as historical data from instrumented seals. A description of data sets and processing is provided in the Methods section. The observations span the years 2007 to 2019, but due spatial variability in the measurement locations, we do not address temporal changes in this study. Shelf properties are consistent with earlier studies of the continental shelf hydrography^{22,28,29}; property distributions are constrained by the lateral circulation over the shelf and, in particular, boundary currents moving towards and away from the coast along the eastern and western edges of glacially-carved troughs, respectively^{22,30}. In the following, we combine the observed hydrographic properties and circulation structure to infer that both surface and subsurface waters are modified through interactions with sea ice and ice shelves. This process likely occurs over much of the WAP and BellS. Steering of the circulation by ice-shelf fronts and large troughs in the Bellingshausen Sea then delivers these waters to the shelf break and leads to an abrupt formation of a westward-flowing ASC in the western BellS.

The distribution of temperature and salinity properties over the continental slope in the BellS (Figure 1, Supp. Figure 2)

reveals an evolution in the frontal structure from west to east. Over most of the continental slope, there is a strong gradient in temperature at the shelf break (a 0.5°C change over less than 20 km, see also Figure 2) associated with the penetration of offshore CDW towards the coast¹⁰. This feature is most prominent at the western side of the BellS and across the mouth of the Belgica Trough (Supp. Figure 2a-d). There are no ship-based observations of the temperature difference at the mouth of the Latady Trough, but this front is much weaker on the eastern side of the trough (Supp. Figure 2f). The properties of the Modified Circumpolar Deep Water (MCDW) are typically attributed to mixing processes occurring as CDW crosses the shelf break, but may also be related to the recirculation of shelf properties within the troughs.

The other major frontal feature apparent in the temperature-salinity distribution occurs in shallower, lighter, density classes and is associated with the presence of subsurface Winter Water (WW) with typical properties $T = -1.85^{\circ}$ C, S = 33.9, $\sigma_0 \approx 27.4$ kg m⁻³, where σ_0 is potential density referenced to the surface. In particular, the western-most transect (Figure 1c) shows a strong salinity difference between lighter offshore waters and saltier onshore waters. The most likley source of this denser form of WW is brine rejection occurring in the large polynyas of the BellS as sea ice forms in late summer and fall³¹ (Supp. Figure 3). While summertime polynyas may cover a substantial fraction of the continental shelf, the saltiest waters are collected and delivered to the shelf break along the western edge of the Belgica Trough by the cyclonic circulation on the shelf²². The temperature gradients of Antarctic Surface Water (AASW), found above WW, also evolve along the shelf break. Waters are warmer in the eastern BellS, under the more direct influence of waters associated with the southern limit of the ACC near the shelf break in the eastern BellS and along the WAP. Farther to the west, surface waters are cold and fresh, sitting close to the surface freezing temperature, consistent with the ACC located further offshore.

Frontal structure in the Bellingshausen Sea

The frontal structure of the western-most cross-slope section (NBP19-01 West) provides information on how the outflow of modified shelf waters interact with the southern boundary of the ACC. Here, the continental shelf has a depth of roughly 500 m although the strongest frontal structure occurs farther offshore roughly near the 1500 m isobath (Figure 2, stations 6-7). Consistent with the temperature-salinity diagrams, the shelf is dominated by cold, relatively salty WW, with the upper 300 m being weakly stratified (low potential vorticity). The density in the upper part of the water column is dominated by salinity. Offshore, unmodified CDW has a maximum temperature close to 2°C, whereas the warmest water found on the shelf here is closer to 1°C, MCDW. Isopycnals that host the warmest water have access to the continental shelf (Figure 2a), but some modification, locally or otherwise, must support this temperature difference. On the shoreward side of offshore CDW core, isopycnal slope downward, away from the shelf break as the salty WW layer impinges into the offshore stratification (Figure 2, stations 6-10); there is a mode of water in the WW density class over the shelf that is not found offshore. Further offshore, deep isopycnals uniformly tilt upward towards the shelf break. This behavior produces a "pinching" in the density surfaces, which may represent an intermittent eddy process in our synoptic section, but more likely indicates a separation between opposing boundary currents.

This second view is supported by both the direct velocity observations and the geostrophic velocities constructed from the density distribution (Figure 2c,d). The shoreward extent of the offshore CDW is associated with an eastward flow (stations 5-6) that is the source of the warm water that enters the Belgica Trough (the maximum depth of the Belgica Trough is ~ 800 m). This eastward flow is sandwiched vertically between a shallow westward flow of surface waters and a deeper westward flow

that extends from 1500 m to the seafloor. Over the continental slope, the eastward core of CDW separates a westward frontal current farther offshore that is likely an extension of the WAP's deep westward boundary current³², and a bottom-intensified westward flow extending from the shoreward edge of the CDW core to the shelf break. We propose that this deep westward flow at the upper continental shelf is the first manifestation of the ASC in the West Antarctic circulation system.

The distinction between the eastward-flowing core of offshore CDW and westward-flowing MCDW, which is modified through interaction with the floating ice shelves in the BellS^{22,30}, is apparent when the distribution of temperature and salinity along this section is colored with the referenced geostrophic velocity (Figure 3a). This analysis also reveals that much of the WW flows eastward, recirculating within the Belgica Trough. While strong property gradients and lateral shear are found between the CDW and MCDW water masses, we argue that the WW properties establish the frontal structure over the upper continental shelf. The shelf's WW is characterized by a weak stratification, an indication of low potential vorticity (PV), since $PV \approx fN^2$ here. The (potential) density classes associated with this WW, roughly 27.4 to 24.6 kg m⁻³, support a strong lateral PV gradient (Figure 3b). Note that the lateral PV gradient over the upper continental slope here differs from the rest of the WAP where density layers shoal and thin towards the shelf break⁹. The PV gradient and the isopycnal slopes support a strong baroclinic flow with a positive vertical shear. The cold and salty WW produces a low (steric) sea surface height anomaly that induces an eastward surface flow³³, and the initiation of the deep westward ASC is due to the thermal wind shear. These dynamics are further highlighted by comparing the cross-slope hydrography and velocity distribution to the east of the Latady Trough (Supp. Figure 4), where lateral gradients are weak and the flow at the shelf break is eastward and largely barotropic.

Discussion

The ASF and the associated ASC have long been identified as primarily a wind-driven phenomena¹⁶. In turn, the impact of the ASC on cross-slope heat transport has also largely focused on wind forcing to explain both temporal^{3,5,19} and spatial^{9,34} variability. Although wind forcing certainly has a key role in setting the frontal structure at the Antarctic margins, the results of the present study provide a more nuanced interpretation of controls on heat transport towards the ice shelves of West Antarctica.

The generation of a sharp frontal structure in the western BellS is related to two distinct water mass transformation processes that occur over the continental shelf. First, observations collected during the JR165 and NB19-01 cruises identify the BellS, and in particular western ice shelves, such as the Venables Ice Shelf, as key sites of melting and thus lightening of relatively warm MCDW on the shelf^{22,30}. This sense of transformation is also consistent with the structure of the overturning circulation in the Amundsen Sea²³ and the BellS²⁹. In contrast, within density classes that are lighter than those hosting the MCDW-to-glacially-modified-CDW transition, sea ice formation leads to the production of relatively dense WW³⁵. This transformation is linked to the large polynyas that are a persistent feature of the numerous bays that populate the southern part of the BellS³¹. Thus water mass modification throughout the BellS is acting to fill volumes that are close in density space and lead to lateral density gradients when these waters are returned to the shelf break (Figure 4).

Another critical component of the west Antarctic circulation is the location of source waters that feed these two transformations in the BellS (Figure 4). It is well documented that the source of warm waters throughout West Antarctica leading to ice shelf melt is the offshore CDW associated with a maximum in temperature ^{15, 22, 36, 37}. Along the WAP, this warm water flows onto the shelf from the southern limit of the ACC, while in the Amundsen Sea, warm CDW also tends to flow from the west before entering the shelf through glacially-carved troughs ^{38, 39}. In the BellS, the core of CDW is also associated with

an eastward flow (Figures 3 and 4) that turns onto the shelf near the center of the Belgica Trough, where the shelf break is at its deepest. The relatively fresh surface water, on the other hand, arrives to the BellS in an extension of the coastal boundary current that is established through the near-surface, coastal injection of fresh water along the WAP: the Antarctic Peninsula Coastal Current (APCC)⁴⁰. There is evidence from modeling simulations⁴¹ and observations³⁰ that the APCC extends into the central Bellingshausen Sea and even strengthens. The APCC has been described as a buoyancy-driven feature⁴⁰, whereas simulations⁴¹ represent the APCC as largely wind-driven; however, the latter did not resolve the freshwater buoyancy forcing at the coast.

The generation of the ASC at the shelf break to the west of the Belgica Trough is likely to be an important mechanism for the transport of water properties towards the Amundsen Sea. The water mass that fills the core of the ASC here is the cumulative result of transformation processes occurring throughout the WAP and Bellingshausen Sea, including sea ice formation, surface heat fluxes, ice shelf melt, and the input of glacial melt. All of these processes are likely to be sensitive to rapid climate changes that have been documented along the WAP^{42–45}. The transmission of changing water properties between basins around Antarctica remains poorly understood⁹. This is particularly critical as major ice shelves in the Amundsen Sea appear to exhibit both "warm cavity" and "cold cavity" regimes that vary over time scales of multiple years⁵. To date, mechanistic explanations for these fluctuations have focused on atmospheric variability⁶. Yet, the integration of physical processes occurring broadly throughout West Antarctica, coupled with advective time scales influenced by boundary currents, may offer further insight into glacial melt rate variability, especially over decadal to centennial timescales.

In this study we report the first direct observations of a westward-flowing ASC in West Antarctica outside of the Amundsen Sea. We propose an initiation mechanism for one of the ocean's major boundary currents that will have a leading role in setting global sea level over the next century. We present evidence that the ASC is not a wind-driven circulation feature in this region, but rather arises from the generation of a density front at the shelf break related to different water mass formation and transformation processes over the continental shelf. The strength of this front, dominated by differences in the WW layer, likely reflects changes in water properties accumulated over the entire BellS and the WAP. Observations of future changes in this westward flow are likely to reflect changes to the WAIS in the WAP and Bellingshausen sectors, while also influencing melt rates of ice shelves located farther to the west.

Methods

The observations analyzed in this study were primarily collected from the R/V Nathaniel B. Palmer (cruise NBP19-01) between December 27, 2018 and January 19, 2019 as part of the TABASCO (Transport of the Antarctic Peninsula and Bellingshausen Sea: Antarctic Slope Current Origins) project. During this period, 56 full-depth CTD stations were occupied over the continental shelf and slope of the Bellingshausen Sea (red dots, Figure 1). These stations were organized into seven transects crossing the major proposed circulation features in this region. CTD data was processed following the guidelines provided by McTaggart et al. $(2010)^{46}$. Full details of the data processing as well as an overview of the water mass properties, circulation strength and structure, heat transport, and the distribution of glacial meltwater in the Bellingshausen Sea are provided in the TABASCO project cruise report, available at http://web.gps.caltech.edu/~andrewt/publications.html.

The CTD stations collected on NBP19-01 are complemented by an extensive hydrographic survey, consisting of 235 full-depth stations, that was completed on the R/V James Clark Ross (cruise JR165) between March 3 and 9 April, 2007 as part

of the ACES-FOCAS project (Antarctic Climate and the Earth System-Forcing from the Oceans, Clouds, Atmosphere and Sea-ice)⁴⁷. Hydrographic stations were undertaken using a Sea-Bird CTD sensor along with a SBE-35 high-precision digital reversing thermometers and two oxygen sensors (CTD-O2 and SBE-43 Oxygen Sensor). Salinity was measured with two conductivity sensors and was calibrated against discrete samples together with the oxygen data. Typical station spacing varied between the transects, but did not exceed 25 km; for transects over the continental shelf, the spacing was as fine as 7 km (Figure 1).

In addition to hydrographic data, Lowered Acoustic Doppler Current Profiles (LADCP) were also collected at all stations on NPB19-01. Prior to using the LADCP data, tidal velocities were analyzed in our region of study using the predicted barotropic tidal currents at each station from the CATS2008 (Circum-Antarctic Tidal Simulation)⁴⁸. Tides were found to be minimal in the Bellingshausen Sea and do not impact our results and interpretation of the LADCP data.

To supplement the ship-based hydrographic data, two ocean gliders were deployed during the NBP 19-01 cruise: one (SG621) on the western side of the Bellingshausen Sea on December 27, 2018 and the other (SG659) along to the Antarctic Peninsula, near Marguerite Trough on January 19, 2019. The gliders sampled until February 20 and March 13, 2019, respectively. Due to sea ice coverage, the gliders had limited access to the continental shelf earlier in the campaign. Therefore we restrict our analysis to data collected by SG539 near the mouth of the Latady Trough as well as over the continental slope to the east of the trough. The gliders collected vertical profiles of temperature and salinity, dissolved oxygen, optical backscatter and fluorescence. Here we focus on the hydrographic data. Temperature and salinity data were collected using a Sea-Bird Electronics CT Sail; temperature and salinity were converted into potential density surfaces using the TEOS-10 toolbox⁴⁹. Effective glider station spacing varied between two and five kilometres on the basis of current speed and water column depth. Conservative temperature, absolute salinity, and the geostrophic shear is calculate using the TEOS-10 toolbox⁴⁹. The definitions of water masses used in this study follow the criteria provided in Jenkins and Jacobs (2008)²⁹.

Finally, we make use of hydrographic data from instrumented elephant seals, which are made available though the MEOP (Marine Mammals Exploring the Oceans Pole to Pole) program⁵⁰. This data is applied to support the formation of a salty version of WW in BellS polynyas over the continental shelf. The data presented in Supplementary Figure 4 is taken from the data set analyzed by Zhang *et al.* $(2016)^{22}$. Details of the data coverage in both space and time, as well as processing techinques, are described in this manuscript.

References

- 1. Paolo, F., Fricker, H. & Padman, L. Volume loss from Antarctic ice shelves is accelerating. Science 348, 327–331 (2015).
- 2. Pritchard, H. D. et al. Antarctic ice-sheet loss driven by basal melting of ice shelves. Nature 484, 502–505 (2012).
- 3. Dutrieux, P. et al. Strong sensitivity of Pine Island ice-shelf melting to climatic variability. Science 343, 174–178 (2014).
- **4.** Whitworth, T., Orsi, A. H., Kim, S.-J., Nowlin, W. D. & Locarnini, R. A. Water masses and mixing near the Antarctic Slope Front. In Ray, S. S. & Weiss, F. (eds.) *Ocean, ice, and atmosphere: interactions at the Antarctic continental margin*, vol. 75 of *Antarctic Research Series*, 1–27 (American Geophysical Union, 1998).
- **5.** Jenkins, A. *et al.* West Antarctic Ice Sheet retreat in the Amundsen Sea driven by decadal oceanic variability. *Nat. Geosci.* **11**, 733–738 (2018).

- **6.** Holland, P. R., Bracegirdle, T. J., Dutrieux, P., Jenkins, A. & Steig, E. J. West Antarctic ice loss influenced by internal climate variability and anthropogenic forcing. *Nat. Geosci.* **12**, 718–724 (2019).
- 7. Donat-Magnin, M. *et al.* Ice-shelf melt response to changing winds and glacier dynamics in the Amundsen Sea sector, Antarctica. *J. Geophys. Res.* **122**, 10206–10224 (2017).
- **8.** Webber, B. G. M. *et al.* Mechanisms driving variability in the ocean forcing of Pine Island Glacier. *Nat. Comm.* **8**, 14507 (2017).
- **9.** Thompson, A. F., Stewart, A. L., Spence, P. & Heywood, K. J. The Antarctic Slope Current in a changing climate. *Rev. Geophys.* **56**, 741–770 (2018).
- **10.** Jacobs, S. S. On the nature and significance of the Antarctic Slope Front. *Mar. Chem.* **35**, 9–24 (1991).
- **11.** Stewart, A. L., Klocker, A. & Menemenlis, D. Circum-Antarctic shoreward heat transport derived from an eddy- and tide-resolving simulations. *Geophys. Res. Lett.* **45**, 834–845 (2018).
- **12.** Moffat, C., Owens, B. & Beardsley, R. C. On the characteristics of Circumpolar Deep Water intrusions to the west Antarctic Peninsula continental shelf. *J. Geophys. Res.* **114**, C05017 (2009).
- **13.** Walker, D. P., Jenkins, A., Assmann, K. M., Shoosmith, D. R. & Brandon, M. A. Oceanographic observations at the shelf break of the Amundsen Sea, Antarctica. *J. Geophys. Res. Ocean.* **118**, 2906–2918 (2013).
- **14.** Nakayama, Y., timmermann, R., Rodehacke, C. B., Schröder, M. & Hellmer, H. H. Modeling the spreading of glacial meltwater from the Amundsen and Bellingshausen Seas. *Geophys. Res. Lett.* **41**, 7942–7949 (2014).
- **15.** Nakayama, Y., Menemenlis, D., Zhang, H., Schodlok, M. & Rignot, E. Origin of Circumpolar Deep Water intruding onto the Amundsen and Bellingshausen Sea continental shelves. *Nat. Comm.* **9**, 3403 (2018).
- **16.** Gill, A. E. Circulation and bottom water production in the Weddell Sea. *Deep. Res.* **20**, 111–140 (1973).
- 17. Flexas, M. M., Schodlok, M. P., Padman, L., Menemenlis, D. & Orsi, A. H. Role of tides on the formation of the Antarctic Slope Front at the Weddell-Scotia Confluence. *J. Geophys. Res.* 120, 3658–3680 (2015).
- **18.** Thompson, A. F., Heywood, K. J., Schmidtko, S. & Stewart, A. L. Eddy transport as a key component of the Antarctic overturning circulation. *Nat. Geosci.* **7**, 879–884 (2014).
- **19.** Spence, P. *et al.* Rapid subsurface warming and circulation changes of Antarctic coastal waters by poleward shifting winds. *Geophys. Res. Lett.* **41**, 4601–4610 (2014).
- **20.** Turner, J., Phillips, T., Hosking, J. S., Marshall, G. J. & Orr, A. The Amundsen Sea low. *Int. J. Clim.* **33**, 1818–1829 (2013).
- **21.** Hazel, J. E. & Stewart, A. L. Are the near-antarctic easterly winds weakening in response to enhancement of the Southern Annular Mode? *J. Clim.* **32**, 1895–1918 (2019).
- **22.** Zhang, X., Thompson, A. F., Flexas, M. M., Roquet, F. & Bornemann, H. Circulation and meltwater distribution in the Bellingshausen Sea: From shelf break to coast. *Geophys. Res. Lett.* **43**, 6402–6409 (2016).
- **23.** Webber, B. G. M., Heywood, K. J., Stevens, D. P. & Assmann, K. M. The impact of overturning and horizontal circulation in Pine Island Trough on ice shelf melt in the Eastern Amundsen Sea. *J. Phys. Ocean.* **49**, 63 83 (2019).

- **24.** Fahrbach, E., Rohardt, G. & Krause, G. The Antarctic coastal current in the southeastern Weddell Sea. *Polar Biol.* **12**, 171–182 (1992).
- **25.** Peña-Molino, B., McCartney, M. S. & Rintoul, S. R. Direct observations of the Antarctic Slope Current transport at 113°E. *J. Geophys. Res. Ocean.* **121**, 7390–7407 (2016).
- **26.** Azaneu, M., Heywood, K. J., Queste, B. Y. & Thompson, A. F. Variability of the Antarctic Slope Current system in the northwestern Weddell Sea. *J. Phys. Ocean.* **47**, 2977–2997 (2017).
- 27. Marshall, J. & Speer, K. Closure of the meridional overturning circulation through Southern Ocean upwelling. *Nat. Geosci.*5, 171–180 (2012).
- 28. Talbot, M. H. Oceanic environment of Georget VI ice shelf, Antarctic Peninsula. Ann. Glaciol. 11, 161–164 (1988).
- **29.** Jenkins, A. & Jacobs, S. Circulation and melting beneath George VI ice shelf, Antarctica. *J. Geophys. Res* **113**, C04013 (2008).
- **30.** Ruan, X., Speer, K., Thompson, A. F. & Chretien, L. S. Ice-shelf meltwater overturning in the Bellingshausen Sea. *J. Phys. Ocean.* submitted (2020).
- **31.** Tamura, T., Ohshima, K. I. & Nihashi, S. Mapping of sea ice production for Antarctic coastal polynyas. *Geophys. Res. Lett.* **35**, L07606 (2008).
- **32.** Hillenbrand, C.-D., Grobe, H., Diekmann, B., Kuhn, G. & Fuetterer, D. K. Distribution of clay minerals and proxies for productivity in surface sediments of the Bellingshausen and Amundsen Seas (West Antarctica) Relation to modern environmental conditions. *Mar. Geol.* **193** (2003).
- **33.** Armitage, T. W., Kwok, R., Thompson, A. F. & Cunningham, G. Dynamic topography and sea level anomalies of the Southern Ocean: Variability and teleconnections. *J. Geophys. Res. Ocean.* **123**, 613–630 (2018).
- **34.** Stewart, A. L. & Thompson, A. F. Eddy-mediated transport of warm Circumpolar Deep Water across the Antarctic Shelf Break. *Geophys. Res. Lett.* **42**, 432–440 (2015).
- **35.** Silvano, A. *et al.* Freshening by glacial meltwater enhances melting of ice shelves and reduces formation of Antarctic Bottom Water. *Sci. Adv.* **4** (2018).
- **36.** Moffat, C. & Meredith, M. Shelf–ocean exchange and hydrography west of the Antarctic Peninsula: a review. *Phil. Trans. Roy. Soc. A* **376**, 20170164 (2018).
- 37. Dinniman, M. S. et al. Modeling ice shelf/ocean interaction in Antarctica: A review. Oceanography 29, 144–153 (2016).
- **38.** Walker, D. P. *et al.* Oceanic heat transport onto the Amundsen Sea shelf through a submarine glacial trough. *Geophys. Res. Lett.* **34**, 1–4 (2007).
- **39.** Nakayama, Y., Menemenlis, D., Schodlok, M. & Rignot, E. Amundsen and Bellingshausen Seas simulation with optimized ocean, sea ice, and thermodynamic ice shelf model parameters. *J. Geophys. Res. (published online)* (2017).
- **40.** Moffat, C., Beardsley, R. C., Owens, B. & van Lipzig, N. A first description of the Antarctic Peninsula Coastal Current. *Deep. Res. Pt II* **55**, 277–293 (2008).

- **41.** Holland, P. R., Jenkins, A. & Holland, D. M. Ice and ocean processes in the Bellingshausen Sea, Antarctica. *J. Geophys. Res.* **115**, C05020 (2010).
- 42. Vaughan, D. G. et al. Recent rapid regional climate warming on the Antarctic Peninsula. Clim. Chang. 60, 243–274 (2003).
- **43.** Meredith, M. P. & King, J. C. Rapid climate change in the ocean west of the Antarctic Peninsula during the second half of the 20th century. *Geophys. Res. Lett.* **32**, L19604 (2005).
- **44.** Schmidtko, S., Heywood, K. J., Thompson, A. F. & Aoki, S. Multidecadal warming of Antarctic waters. *Science* **346**, 1227–1231 (2014).
- 45. Cook, A. J. et al. Ocean forcing of glacier retreat in the western Antarctic Peninsula. Science 353, 283–286 (2016).
- **46.** McTaggart, K. E., Johnson, G. C., Johnson, M. C., Delahoyde, F. & and, J. H. S. Notes on CTD/O data acquisition and processing using Sea-Bird hardware and software. IOCCP Reports, Report No. 14 134, ICPO Publication Series (2010).
- **47.** Castro-Morales, K., Cassar, N., Shoosmith, D. R. & Kaiser, J. Biological production in the Bellingshausen Sea from oxygen-to-argon ratios and oxygen triple isotopes. *Biogeosci.* **10**, 2273–2291 (2013).
- **48.** Padman, L., Fricker, H. A., Coleman, R., Howard, S. & Erofeeva, S. A new tidal model for the Antarctic ice shelves and seas. *Ann. Glaciol.* **34**, 247–254 (2002).
- **49.** McDougall, T. J. & Barker, P. M. Getting started with TEOS-10 and the Gibbs Seawater (GSW) Oceanographic Toolbox. Tech. Rep. ISBN 978-0-646-55621-5, SCOR/IAPSO WG127 (2011).
- **50.** Roquet, F. et al. Ocean observations using tagged animals. Oceanography **30**, 139 (2017).
- **51.** Orsi, A. H., Whitworth, T. & Nowlin, W. D. On the meridional extent and fronts of the Antarctic Circumpolar Current. *Deep. Res. Pt. I* **42**, 641–673 (1995).
- **52.** Schaffer, J. *et al.* A global, high-resolution data set of ice sheet topography, cavity geometry, and ocean bathymetry. *Earth Syst. Sci. Data* **8**, 542–557 (2016).

Acknowledgements

We acknowledge the essential contributions from the captain and crew of the R/V Nathaniel B. Palmer as well as the Antarctic Support Contract staff during NBP19-01. We thank A. Jenkins for sharing data from the JR165 cruise. Funding for AFT was provided by OPP-1644172 and the Packard Foundation. Funding for KS was provided by NSF OPP-1643679 and OCE-1658479.

Author contributions statement

All authors contributed to the design of the field program, analysis of the results, and writing of the manuscript.

Additional information

Competing interests The authors declare no competing interests.

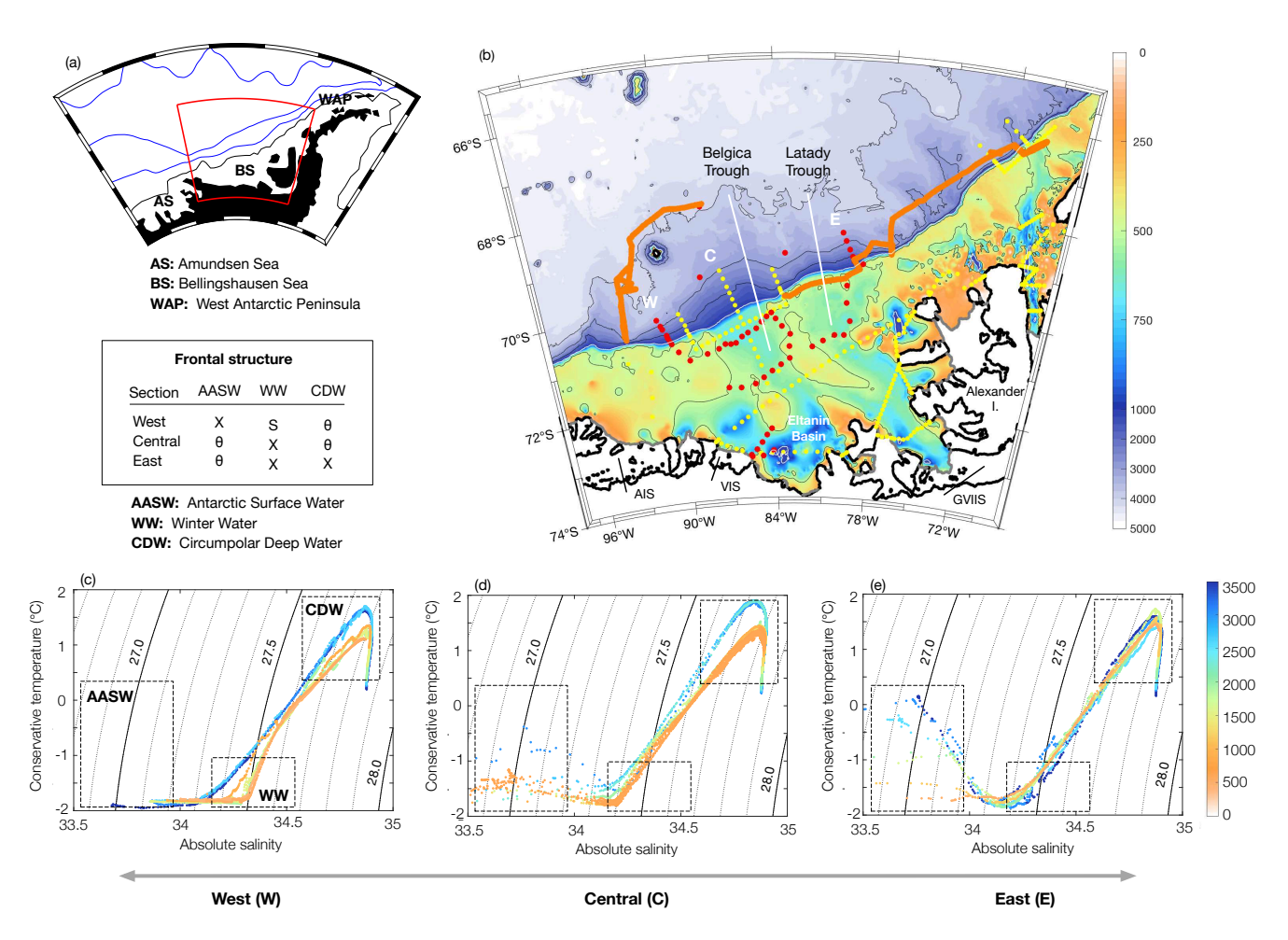


Figure 1. (a) Map of West Antarctica showing the location of the Amundsen and Bellingshausen Seas (AS and BS) and the West Antarctic Peninsula (WAP); the blue curves are the climatological positions of the Antarctic Circumpolar Current's southern fronts⁵¹ and the black curve is the 1000 m isobath. (b) Map of the Bellingshausen Sea corresponding to the red box in panel (a). The bathymetry, given in color, is provided from the RTopo- 2^{52} product. The 500, 2000, 3000, and 4000 m isobaths are contoured in black; the 1000 m isobath, indicative of the position of the shelf break, is contoured in white. Locations of hydrographic profiles collected from cruise JR-165 (yellow), cruise NBP19-01 (red), and gliders deployed during NBP19-01 (orange) are also provided. (Bottom) Temperature-salinity diagrams from the three sections marked as west (W, panel c), central (C, panel d), and east (E, panel e) in the map; the points are colored by the water column depth at the CTD location (note the different color scale to highlight cross-slope variations). Contours show potential density (σ_0), at 0.1 kg m⁻³ intervals. Density classes indicating Antarctic Surface Water (AASW), Winter Water (WW), and Circumpolar Deep Water (CDW) are highlighted by boxes in each panel. The table indicates water masses that exhibit fronts (abrupt shifts in water properties) in each of the three sections; Θ, S and X indicate a temperature front, a salinity/density front or absence of a front, respectively.

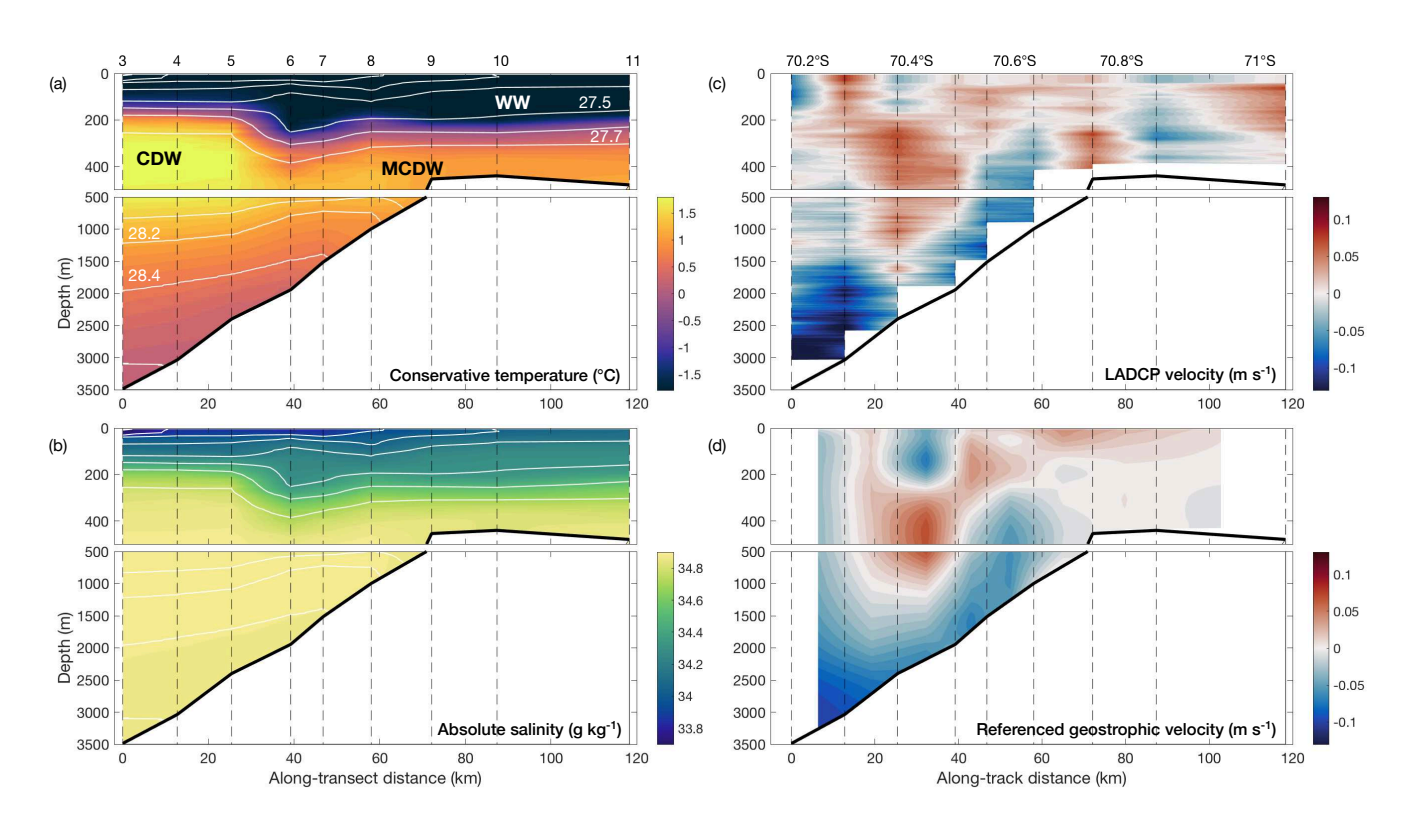


Figure 2. Cross-slope section located to the west of the Belgica Trough from NBP19-01 (section W in Figure 1): (a) Conservative Temperature (°C), (b) Absolute Salinity (g kg⁻¹), (c) across-transect velocity from the lowered acoustic Doppler current profiler (LADCP) (m s⁻¹), (d) geostrophic velocity referenced to the LADCP (m s⁻¹). In panels (a) and (b) the contours show potential density σ_0 with contours intervals of 0.1 kg m⁻³ between 27 and 27.8 kg m⁻³ and intervals of 0.02 kg m⁻³ between 27.8 and 27.86 kg m⁻³. In panels (c) and (d), positive and negative (red and blue) velocities indicate eastward and westward flow, respectively. The thick black curve shows the depth of the seafloor while the dashed curves indicate the positions of individual CTD casts (corresponding to stations 3-11). Station numbers are listed above panel (a), latitude is listed above panel (c). Key water masses (CDW = Circumpolar Deep Water, MCDW = Modified Circumpolar Deep Water, WW = Winter Water) are shown in panel (a).

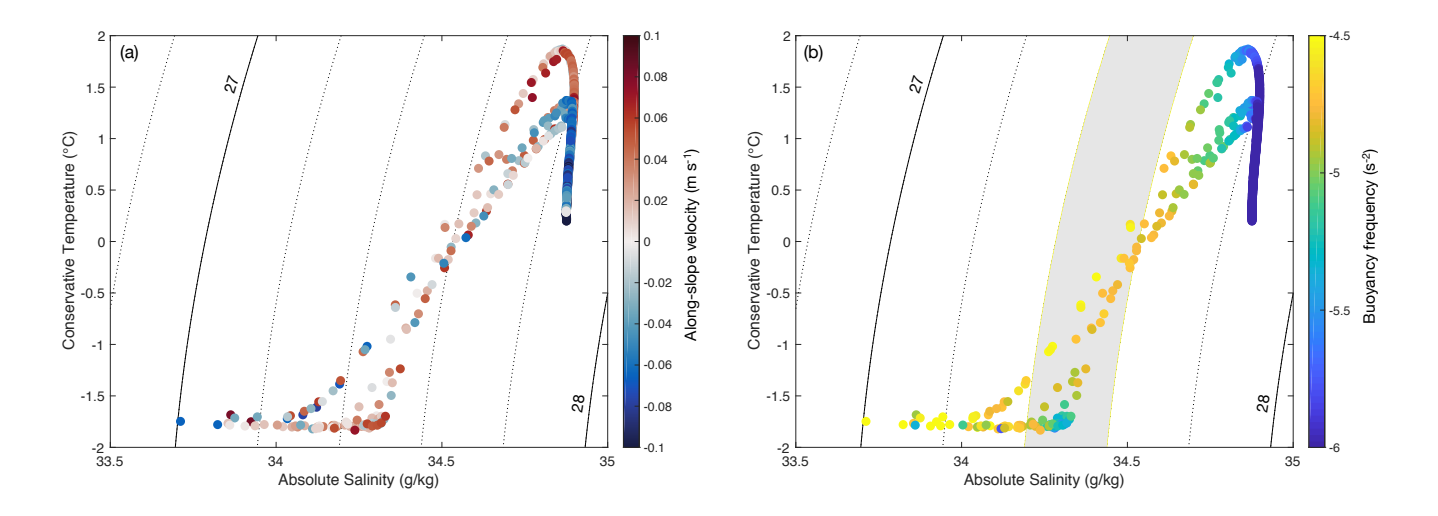


Figure 3. Conservative temperature-absolute salinity diagram colored by: (a) along-slope velocity (m s⁻¹) and (b) buoyancy frequency N^2 (s⁻²). The black contours are potential density referenced to the surface, σ_0 ; contour intervals are 0.2 kg m⁻³. The left hand panel shows that the strongest core of eastward flow is located offshore and is comprised of Circumpolar Deep Water (CDW), while the westward flow is closer to the shelf break. Eastward flow is located within the on-shore Winter Water (WW) water mass. The right hand panel is a proxy for potential vorticity as $PV \approx fN^2$. The color scale is logarithmic, such that $-6 = 10^{-6}$. The on-shore WW layer stands out as a region of particularly low PV, or weak stratification. The shaded region highlights a band of isopcynals where a strong isopycnal PV gradient is maintained due to the low-PV WW. This PV gradient supports a strong baroclinic flow with the thermal wind shear supporting the deep westward ASC.

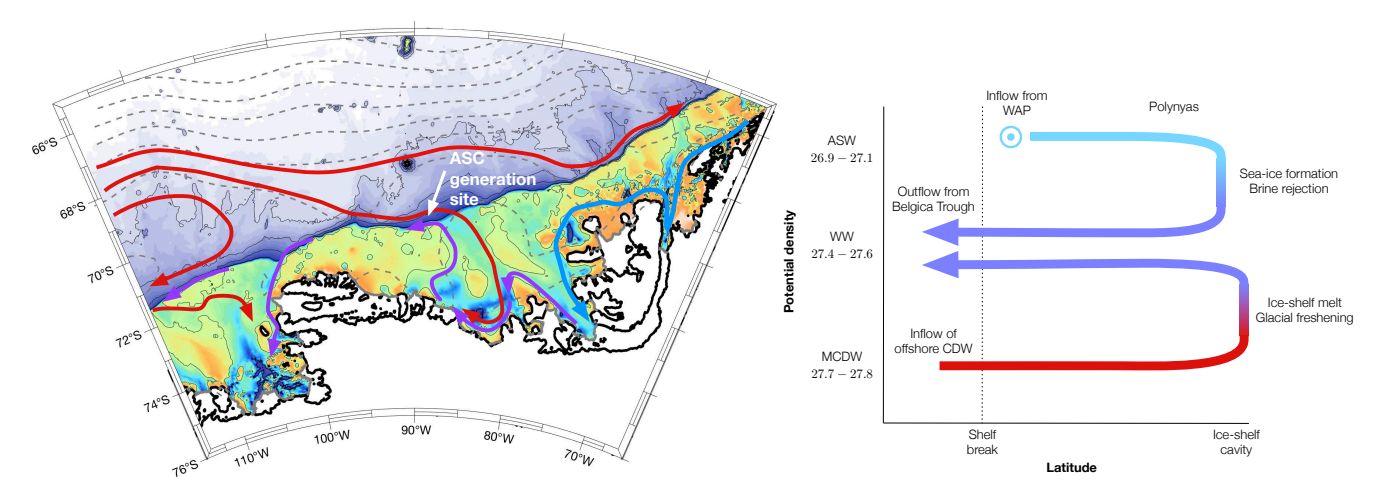
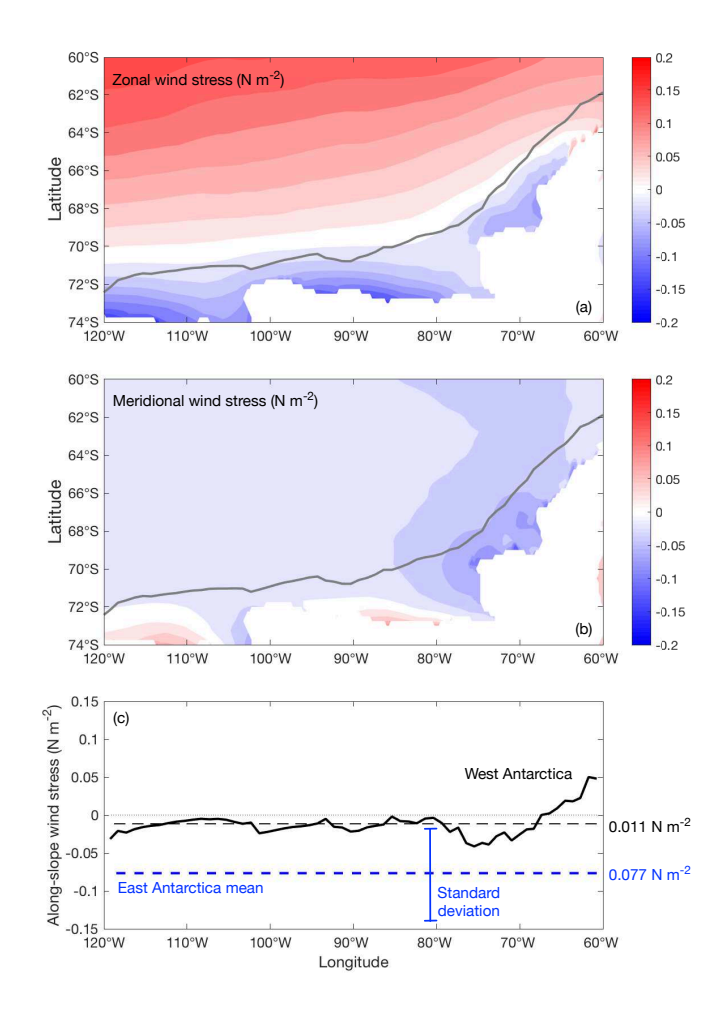
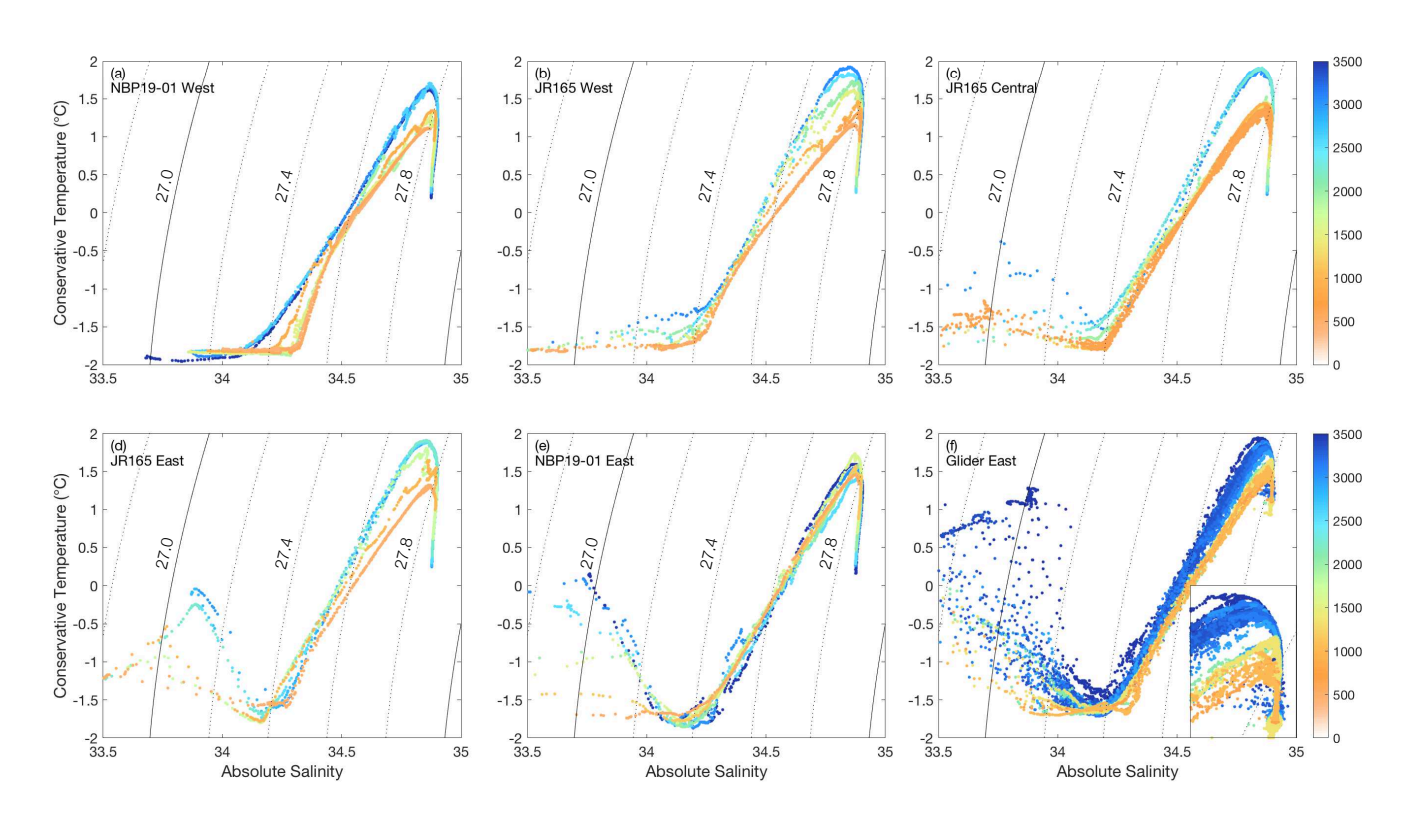


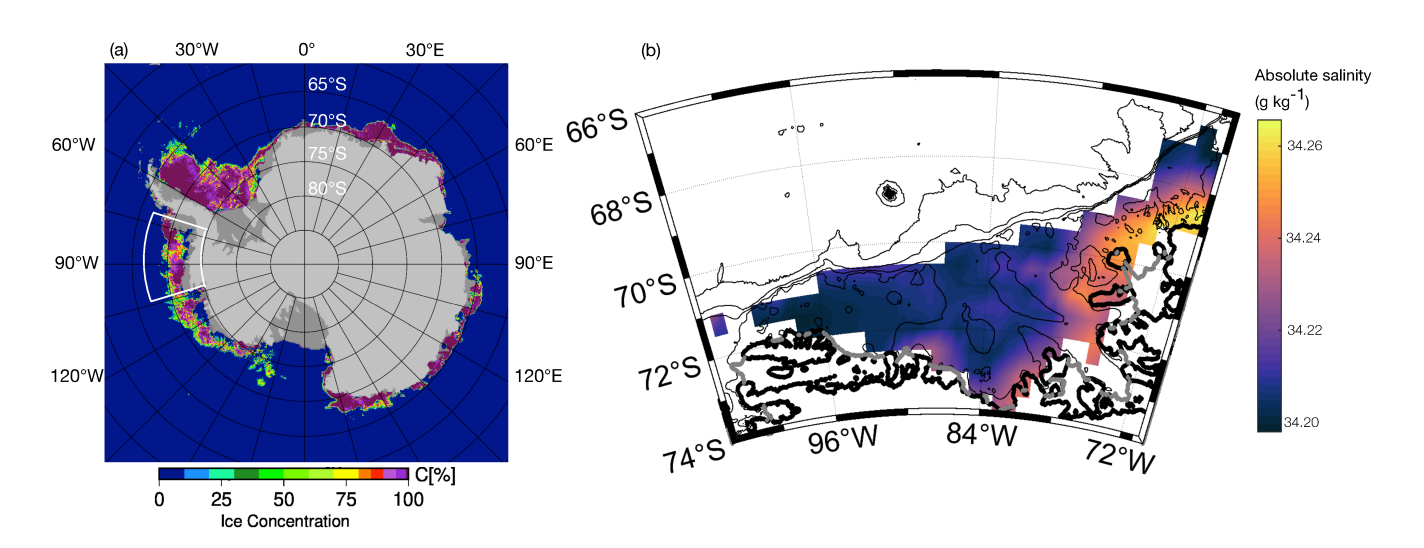
Figure 4. (Left) Schematic depiction of transport pathways in the Bellingshausen and Amundsen Seas that give rise to the generation of the ASC on the western edge of the Belgica Trough. Colors indicate bathymetry using the same colorbar as in Figure 1. The dashed gray lines show the mean dynamic topography from 2011-2016³³ at intervals of 5 cm. Colors of the arrows indicate the dominant water mass carrying the transport as indicated in the right-hand panel. (Right) Diagram of the water transformation processes that fill the Winter Water (WW) density class and generate the frontal structure at the shelf break when this water mass is exported from the shelf.



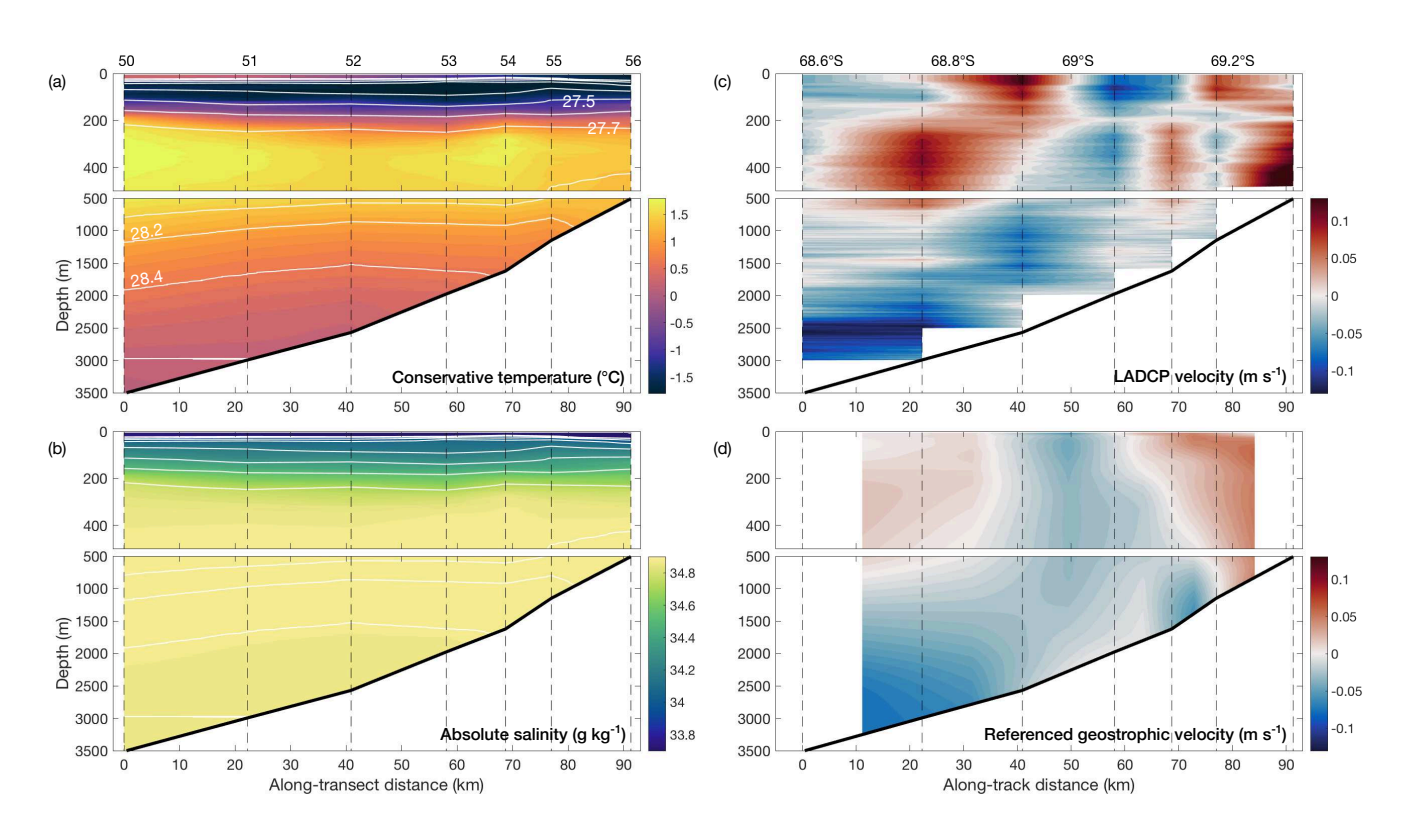
Supplementary Figure 1: Multidecadal mean (a) zonal and (b) meridional wind stress (N m⁻²) in West Antarctica from 1979-2014 ERA-Interim. (c) Multidecadal along-slope wind stress evaluated along the 1000 m isobath, indicative of the shelf break (black curve). Mean along-slope wind stress at the 1000 m isobath is indicated by the dashed lines for West Antarctica (120°W to 60°W, black) and East Antarctica (all other longitudes, blue). The standard deviations of the along-slope wind stress outside of West Antarctica is also provided (blue vertical line). Figure modified from Fig. 1 of Hazel and Stewart (2019)²¹.



Supplementary Figure 2: Conservative temperature-absolute salinity diagrams for all of the cross-slope sections depicted in Figure 1b. The panels are organized from west to east, and were collected from NBP19-01 (panels a, e; red dots in Figure 1), JR165 (panels b, c, d, yellow dots in Figure 1), and from an ocean glider deployed in 2019 (panel f; orange dots in Figure 1) (Methods). The points are colored by the water column depth at the CTD locations. Contours show potential density (σ_0), at 0.2 kg m⁻³ intervals. Panels (a), (c) and (e) are repeated from Figure 1 for clarity. The diagrams show distinct progressions in frontal structure in three different density classes: (i) Antarctic Surface Water (AASW) become warmer and fresher with more lateral variability moving west to east; (ii) Winter Water (WW) shows an abrupt transition or front in salinity in the westernmost section (a) but is weaker everywhere to the east; (iii) a front in Circumpolar Deep Water (CDW) is apparent across most of the Belgica Trough (panels (a-d), but disappears or is weak to the east of Latady Trough (panels e,f).



Supplementary Figure 3: (a) Antarctic sea ice concentration from January 20, 2019. This distribution is indicative of climatological distributions and shows large polynyas in the southern Bellingshausen Sea. (b) Distribution of absolute salinity (g kg⁻¹) for the region indicated in white in panel (a), based on data collected by instrumented seals between 2007 and 2014^{22,50}. The salinity has been interpolated on to the $\sigma_0 = 27.4$ kg m⁻³ density surface, which is associated with Winter Water (Fig. 1, Suppl. Figure 2). Coastal regions that are populated by large polynyas most years³¹, are shown to be elevated in salinity, which suggests regions of sea ice formation and brine rejection.



Supplementary Figure 4: Cross-slope section located to the east of the Latady Trough from NBP19-01 (section E in Figure 1): (a) Conservative Temperature (°C), (b) Absolute Salinity (g kg⁻¹), (c) across-transect velocity from the lowered acoustic Doppler current profiler (LADCP) (m s⁻¹), (d) geostrophic velocity referenced to the LADCP (m s⁻¹). In panels (a) and (b) the contours show potential density σ_0 with contours intervals of 0.1 kg m⁻³ between 27 and 27.8 kg m⁻³ and intervals of 0.02 kg m⁻³ between 27.8 and 27.86 kg m⁻³. In panels (c) and (d), positive and negative (red and blue) velocities indicate eastward (retrograde) and westward (prograde) flow, respectively. The thick black curve shows the depth of the seafloor while the dashed curves indicate the positions of individual CTD casts (corresponding to stations 50-56). Station numbers are listed above panel (a); latitude is listed above panel (c).